Decomposition Reactions and Reversibility of the $LiBH_4-Ca(BH_4)_2$ Composite

Ji Youn Lee,[†,||] Dorthe Ravnsbæk,[‡] Young-Su Lee,[*,†] Yoonyoung Kim,[†] Yngve Cerenius,[§] Jae-Hyeok Shim,[†] Torben R. Jensen,[‡] Nam Hwi Hur,[||] and Young Whan Cho[†]

Materials Science and Technology Research Division, Korea Institute of Science and Technology, Seoul 136-791, Republic of Korea, Interdisciplinary Nanoscience Center (iNANO) and Department of Chemistry, Langelandsgade 140, University of Aarhus, DK-8000, Denmark, MAX-lab, Lund University, S-22100, Lund, Sweden, and Department of Chemistry, Sogang University, Seoul 121-742, Republic of Korea

Received: May 12, 2009; Revised Manuscript Received: June 21, 2009

$LiBH_4$ is one of the promising candidates for hydrogen storage materials because of its high gravimetric and volumetric hydrogen capacity. However, its high dehydrogenation temperature and limited reversibility has been a hurdle for its use in real applications. In an effort to overcome this barrier and to adjust the thermal stability, we make a composite system $LiBH_4-Ca(BH_4)_2$. In order to fully characterize this composite system we study $xLiBH_4 + (1 - x)Ca(BH_4)_2$ for several x values between 0 and 1, using differential scanning calorimetry, in situ synchrotron X-ray diffraction, thermogravimetric analysis, and mass spectrometry. Interestingly, this composite undergoes a eutectic melting at ca. 200 °C in a wide composition range, and the eutectic composition lies between $x = 0.6$ and 0.8. The decomposition characteristics and the hydrogen capacity of this composite vary with x, and the decomposition temperature is lower than both the pure $LiBH_4$ and $Ca(BH_4)_2$ at intermediate compositions, for example, for $x \approx 0.4$, decomposition is finished below 400 °C releasing about 10 wt % of hydrogen. Partial reversibility of this system was also confirmed for the first time for the case of a mixed borohydride composite.

1. Introduction

Complex metal hydrides hold a great promise as potential solid state hydrogen storage materials because of their high theoretical hydrogen storage capacity.[1,2] Within this class of materials, $LiBH_4$ is one of the most studied case since it has a hydrogen content of 18.5 wt % and the following reversible reaction can release as much as 13.9 wt % hydrogen:

$$LiBH_4 \leftrightarrow LiH + B + 3/2H_2 \qquad 13.9\ \text{wt \%}\ H_2 \quad (1)$$

Practical use of $LiBH_4$ however has been hampered due to its high dissociation temperature,[3] and therefore various strategies have been pursued to lower its decomposition temperature such as adding catalysts,[4,5] confinement in a nanoporous scaffold,[6,7] and destabilization using metal or metal hydrides.[8−10] Another route to adjust stability is to mix with less stable metal borohydrides. A systematic study by Nakamori et al.[11] has shown that stability of metal borohydrides can be roughly estimated by the electronegativity of cation; a less electronegative metal can form a more stable metal borohydride. According to this principle, stability of a mixed borohydride $LiBH_4$-$M(BH_4)_n$ can be tuned by changing the metal M and the mixing ratio. To our knowledge, M = Zn,[12] Al, Zr,[13] K,[14,15] and Sc[16,17] have been investigated so far. Li et al.[13] characterized the thermal decomposition behavior of M = Zn, Al, and Zr. In the case of Zn and Al, separation into the two individual borohydrides occurs upon heating, but the decomposition temperature of $ZrLi_{m-4}(BH_4)_m$ ($m = 5, 6$) lies between that of pure $Zr(BH_4)_4$ and $LiBH_4$, which could validate this approach as a means of adjusting thermodynamics of complex metal hydride. Nickels et al. reported a similar trend in their recent study on $LiK(BH_4)_2$.[14]

These previous studies underscore the need for further investigation on multiple-cation borohydrides. However, in order to design novel mixed cation borohydrides, knowledge of the underlying mechanism for the changes in stability due to varying cation composition must be understood. In some of the aforementioned double-cation borohydrides, even the starting phases were not well characterized not to mention the decomposition product; to the best of our knowledge reversibility has never been reported.

Here we pursue a more practical approach inspired by recent studies which have proved the reversibility of the following reactions[18−21]

$$6LiBH_4 + CaH_2 \leftrightarrow 6LiH + CaB_6 + 10H_2 \qquad 11.7\ \text{wt \%}\ H_2 \quad (2)$$

$$Ca(BH_4)_2 \leftrightarrow 2/3CaH_2 + 1/3CaB_6 + 3H_2 \qquad 9.6\ \text{wt \%}\ H_2 \quad (3)$$

Both reaction schemes 2 and 3 promise large hydrogen storage capacity, but even higher in their combination as the following:

$$4LiBH_4 + Ca(BH_4)_2 \leftrightarrow 4LiH + CaB_6 + 10H_2 \qquad 12.8\ \text{wt \%}\ H_2 \quad (4)$$

A pseudobinary system as shown in eq 4 has the potential to form intermediate compounds, solid solution, or can remain as

* To whom correspondence should be addressed. E-mail: lee0su@kist.re.kr.
† Korea Institute of Science and Technology.
‡ University of Aarhus.
§ Lund University.
|| Sogang University.

10.1021/jp904400b CCC: $40.75
Published on Web 07/22/2009

a physical mixture of two solids, $LiBH_4$ and $Ca(BH_4)_2$. Therefore, a systematic study of the composite $xLiBH_4 + (1 - x)Ca(BH_4)_2$ was performed. Scanning through wide composition ranges will provide a clear picture of the initial phases. Second, we would like to address whether reaction 4 precedes reactions 2 and 3. In that case, $LiBH_4$ and $Ca(BH_4)_2$ would react directly and the composite system would exhibit lower stability than the pure compounds $LiBH_4$ and $Ca(BH_4)_2$. Lastly, the reversibility of the composite system will also be discussed.

2. Experimental Section

2.1. Starting Material. $LiBH_4$ (assay 95%, Acros), $Ca(BH_4)_2 \cdot 2THF$ (assay 98%, Sigma-Aldrich), and NbF_5 (assay 98%, Sigma-Aldrich) were used as starting materials. Adduct-free $Ca(BH_4)_2$ was prepared by drying the commercial powder at around 200 °C in vacuum for 20 h, and $LiBH_4$ and NbF_5 powders were used as-purchased. The powders were handled in an argon-filled glovebox (LABstar, MBraun, $p(O_2, H_2O) < 1$ ppm).

Each batch of composite was about 2 g of $LiBH_4$ and $Ca(BH_4)_2$ mixture in different molar ratio of x:1−x, $x = 0.9$, 0.8, 0.7, 0.6, 0.5, 0.4, 0.2. The powder composite was placed in a hardened steel bowl with seven 12.7 mm and fourteen 7.9 mm diameter Cr-steel, which was then sealed with a Viton O-ring and a lid. The ball-milling was conducted using a planetary mill (Fritsch P7) at 600 rpm for 4 h. For $x = 0.4$, $0.4LiBH_4 + 0.6Ca(BH_4)_2 + 0.02NbF_5$ (in molar ratio) were prepared in the same manner.

The phase composition of as-milled samples were investigated with laboratory X-ray diffraction (XRD, Bruker D8 with Cu Kα radiation, $\lambda = 1.5418$ Å). All laboratory XRD measurements were performed at room temperature. A dome-shaped, vacuum tight, sample holder was used to prevent contact with air during XRD measurement.

2.2. Thermal Analysis. Differential scanning calorimetry (Netzsch DSC 204 F1), thermogravimetric analysis (Netzsch TG 209 F1), and mass spectrometry (Netzsch QMS 403 C) were carried out to analyze the dehydrogenation path of the samples. For differential scanning calorimetry (DSC) and thermogravimetric analysis (TGA), ca. 3 mg of sample was used; data were recorded while heating to 500 °C at a scanning rate of 2 °C/min under flowing argon condition (assay 99.9999%, 50 mL/min).

2.3. In Situ Synchrotron XRD. In situ synchrotron radiation power X-ray diffraction (SR-PXD) measurements were carried out at the synchrotron MAX II, Lund, Sweden, in the research laboratory MAX-Lab at beamline I711 with a MAR165 CCD detector system.[22] The selected X-ray wavelength was 1.09801 Å. The sample cell was specially developed for studies of gas/solid reactions and allows high pressure and temperature to be applied. The samples were mounted in a sapphire single crystal tube (1.09 mm o.d., 0.79 mm i.d., Al_2O_3) in an argon filled glovebox $p(O_2, H_2O) < 0.1$ ppm. The temperature was controlled with a thermocouple placed in the sapphire tube next to the sample. A gas supply system was attached to the sample cell, which allows change of gas and pressure via a vacuum pump during X-ray data acquisition. The details of the experimental setup can be found in ref 23. The system was flushed with Ar and evacuated three times before the valve to the sample was opened prior to the X-ray experiment. The X-ray exposure time was 30 s (2 × 15 s) per powder diffraction pattern. All the in situ dehyderogenation experiments were done at a scanning rate of 2 °C/min under $p(H_2) = 1$ bar unless otherwise mentioned. The FIT2D program was used to remove diffraction spots from the sapphire sample holder.[24]

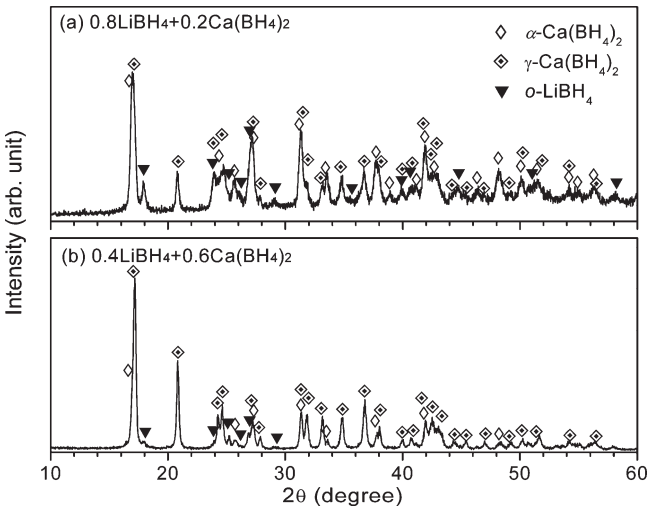

Figure 1. X-ray diffraction (XRD) patterns of the as-milled $xLiBH_4 + (1 - x)Ca(BH_4)_2$ samples, (a) $x = 0.8$ (b) $x = 0.4$. The two samples are physical mixtures of $LiBH_4$ and $Ca(BH_4)_2$.

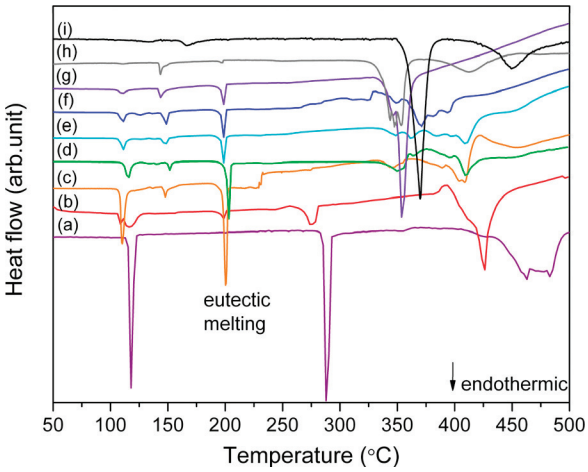

Figure 2. DSC curves for the composites $xLiBH_4 + (1 - x)Ca(BH_4)_2$. (a) $x = 1$, (b) 0.9, (c) 0.8, (d) 0.7, (e) 0.6, (f) 0.5, (g) 0.4, (h) 0.2, (i) 0. The melting point of $LiBH_4$ around 280 °C shifts down to ca. 200 °C when mixed with $Ca(BH_4)_2$. The endothermic peak at ca. 110 °C is a polymorphic phase transition of $LiBH_4$ from *o*-$LiBH_4$ to *h*-$LiBH_4$, and several peaks around 150 °C correspond to the phase transitions of $Ca(BH_4)_2$.

3. Results and Discussion

3.1. Starting Material. Figure 1 shows XRD pattern of two composites ($x = 0.8$ and 0.4) after milling. All observed reflections are identified as a polymorph of $Ca(BH_4)_2$ or $LiBH_4$, and shift in peak positions is only insignificant compared to the two pure borohydrides. Hence we conclude that $LiBH_4$ or $Ca(BH_4)_2$ exist as a physical mixture rather than a new compound or a solid solution. Interestingly, ball-milling with $LiBH_4$ gives a mixture of α-$Ca(BH_4)_2$[25] and γ-$Ca(BH_4)_2$,[26,27] but no Bragg reflection can be assigned to β-$Ca(BH_4)_2$[26] which is usually the majority phase of the $Ca(BH_4)_2$ powder dried at 200 °C.[28]

3.2. Thermal Analysis. We present in Figure 2 the DSC data of $xLiBH_4 + (1 - x)Ca(BH_4)_2$ composite at nine different values of x. DSC data verify the XRD data that these two borohydrides remain unaffected by each other in the as-milled samples under the conditions studied. The polymorphic transformation from orthorhombic (*o*-$LiBH_4$) to hexagonal (*h*-$LiBH_4$) $LiBH_4$ at ca. 110 °C, and several endothermic peaks around 150 °C related to those of $Ca(BH_4)_2$ are consistently observed independent of

the composition. However, a thermal event is observed for the composite, an endothermic peak at 200 °C, which is not observed for either pure $LiBH_4$ or $Ca(BH_4)_2$. The appearance of this peak accompanies the disappearance of the peak for the melting of $LiBH_4$ at 280 °C (except for $x = 0.9$).[29] From a typical phase diagram of pseudobinary system having negligible mutual solubility, we suspect that the endothermic peak at 200 °C would arise from the eutectic melting of $LiBH_4$ and $Ca(BH_4)_2$. This hypothesis has been thoroughly investigated by *in situ* SR-PXD measurements, which is presented in Section 3.3.2.

DSC results raise another interesting point. For composites rich in either $LiBH_4$ or $Ca(BH_4)_2$, the decomposition proceeds in multiple steps and occurs above 400 °C, that is, the excess amounts decomposes like pure $LiBH_4$ or $Ca(BH_4)_2$. Second, the DSC curves for the intermediate compositions cannot be accounted for by a simple overlap of $x = 0$ and $x = 1$, a certain kind of chemical reaction should occur between $LiBH_4$ and $Ca(BH_4)_2$ during decomposition. Furthermore, DSC data implies that $x = 0.8$ is not an optimal composition in order to reduce the decomposition temperature. In fact, the lowest decomposition temperature was achieved at $x = 0.4$ where a major decomposition ends at only 370 °C. This is in contrast to our expectation from reaction 4.

3.3. In Situ XRD Experiment. ***3.3.1. Polymorphic Phase Transition of $Ca(BH_4)_2$.*** While structure and transition between different polymorphs of $LiBH_4$ is well understood, those of $Ca(BH_4)_2$ seem much more complicated and are still not fully understood.[30,31] Five different polymorphs of $Ca(BH_4)_2$ have been reported up to now. At room temperature, mixtures of α-, β-, and γ-$Ca(BH_4)_2$ are usually found and the proportion of each phase is very sensitive to the preparation condition.[26,32−36] Several in situ XRD experiments have shown that α- and γ-$Ca(BH_4)_2$ transform to β-$Ca(BH_4)_2$ upon increasing temperature. Theoretical work based on density functional theory[26,27,37] supports this experimental observation that α-$Ca(BH_4)_2$ is stable at low temperatures and β-$Ca(BH_4)_2$ at elevated temperatures. Majzoub et al.[27] predicted that γ-$Ca(BH_4)_2$ is metastable, but this point has not been proven experimentally. Another polymorph δ-$Ca(BH_4)_2$ reported by Riktor et al.[32,38] appears at higher temperatures than β-$Ca(BH_4)_2$. No structural information has yet been given for δ-$Ca(BH_4)_2$. Filinchuk et al.[36] recently identified another polymorph α′-$Ca(BH_4)_2$ which forms from α-$Ca(BH_4)_2$ via a second-order phase transition and transforms to β-$Ca(BH_4)_2$ at elevated temperature.

In our composite system, we clearly observed α-$Ca(BH_4)_2$ → γ-$Ca(BH_4)_2$ → β-$Ca(BH_4)_2$ transition in a narrow temperature range of ca. 30 °C as shown in Figure 3 for $x = 0.8$. The same sequential phase transition was observed at other x values not presented here. This rapid transition is in contrast to the similar but rather slow transition in the case of pure $Ca(BH_4)_2$[32,36] in which α- to γ-$Ca(BH_4)_2$ transition has never been reported. This may suggest that a tiny amount of $LiBH_4$ is dissolved in the $Ca(BH_4)_2$ lattice and the phase transition is facilitated by the created lattice defects. Our result could tell which polymorph is thermodynamically most stable at a given temperature provided that the presence of $LiBH_4$ does not affect the relative stability of these three polymorphs.

3.3.2. Eutectic Melting. We performed in situ SR-PXD measurements for $x = 0.9$, 0.8, 0.6, 0.5, and 0.4. The eutectic melting predicted by DSC data is consistently observed, and the in situ SR-PXD data locate the eutectic composition between $x = 0.6$ and 0.8. SR-PXD patterns at ca. 200 °C for $x = 0.8$ and 0.6 are plotted in Figure 4 and Figure 5, respectively. These

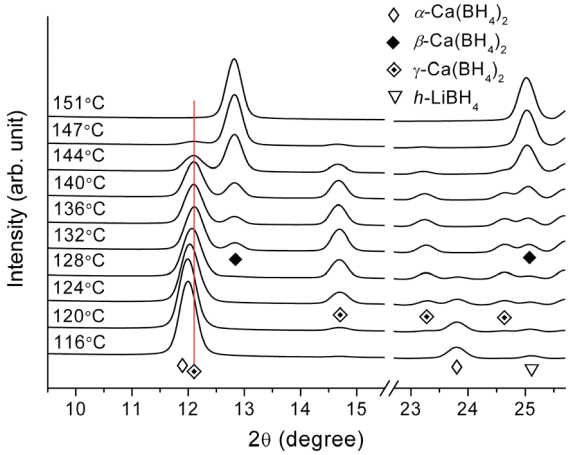

Figure 3. In situ SR-PXD patterns of $0.8LiBH_4 + 0.2Ca(BH_4)_2$ as a function of temperature upon heating at 2 °C/min. Polymorphic phase transitions from α-$Ca(BH_4)_2$ to γ-$Ca(BH_4)_2$ and to β-$Ca(BH_4)_2$ are clearly seen. The main peaks of α-$Ca(BH_4)_2$ and γ-$Ca(BH_4)_2$ overlap around 12°, but as the proportion of γ-$Ca(BH_4)_2$ increases the peak position shifts toward higher angle where the main peaks of γ-$Ca(BH_4)_2$ are located. Above 150 °C, $Ca(BH_4)_2$ exists in the β-$Ca(BH_4)_2$ form.

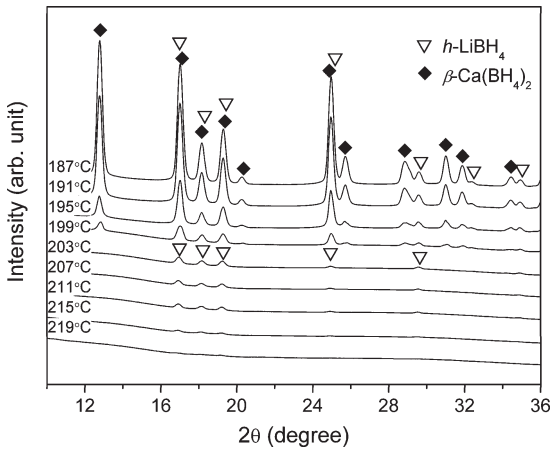

Figure 4. In situ SR-PXD patterns of $0.8LiBH_4 + 0.2Ca(BH_4)_2$ as a function of temperature upon heating at 2 °C/min. β-$Ca(BH_4)_2$ becomes a complete melt at around 200 °C and then h-$LiBH_4$ melts at around 220 °C.

SR-PXD patterns provide a direct evidence of the eutectic melting; as temperature increases, β-$Ca(BH_4)_2$ disappears first in Figure 4 whereas h-$LiBH_4$ disappears first in Figure 5. We provide in Figure 6 a schematic phase diagram of this pseudobinary system for clarity. Two dots in the diagram indicate the temperature at which the remaining solid compound, $LiBH_4$ or $Ca(BH_4)_2$, disappears from the SR-PXD pattern and that could be an upper limit of the liquidus temperature (drawn in dashed line). In the case of $x = 0.6$, β-$Ca(BH_4)_2$ transforms to δ-$Ca(BH_4)_2$ almost simultaneously with the eutectic melting, and the temperature marked in Figure 6 corresponds to the temperature at which δ-$Ca(BH_4)_2$ disappears. Here δ-$Ca(BH_4)_2$ appears at temperatures at more than 100 °C lower than the case of pure $Ca(BH_4)_2$,[32,38] which again hints at a rapid phase transformation in this composite system. In the case of $x = 0.8$, δ-$Ca(BH_4)_2$ was not observed probably because $Ca(BH_4)_2$ melts completely before the β- to δ-$Ca(BH_4)_2$ transition starts.

3.3.3. Decomposition Process. In situ SR-PXD data reveals the complexity of the decomposition reaction for the composites investigated here, which is clearly illustrated in Figure 7 and Figure 8 for the composites $x = 0.8$ and 0.6 in the temperature up to 550 °C.

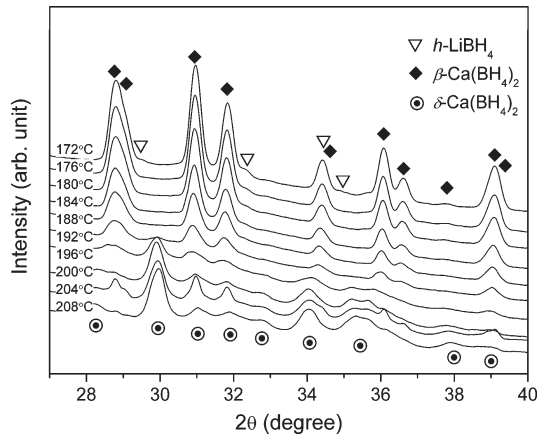

Figure 5. In situ SR-PXD patterns of $0.6LiBH_4 + 0.4Ca(BH_4)_2$ as a function of temperature. *h*-$LiBH_4$ becomes a complete melt at around 200 °C. The remaining β-$Ca(BH_4)_2$ transforms to δ-$Ca(BH_4)_2$.

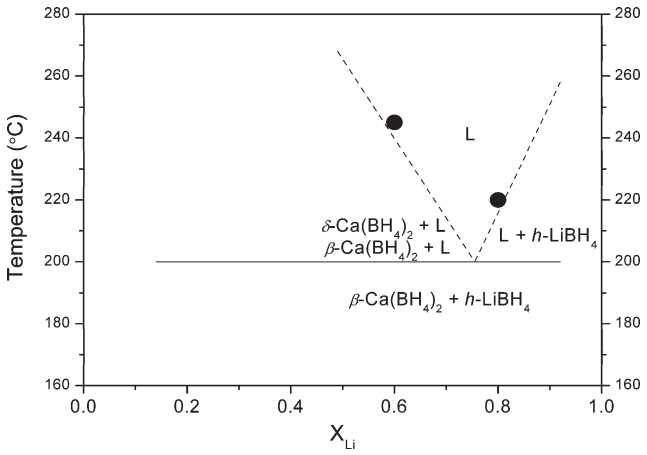

Figure 6. Schematic phase diagram for pseudobinary composite $xLiBH_4 + (1 - x)Ca(BH_4)_2$ around the eutectic temperature.

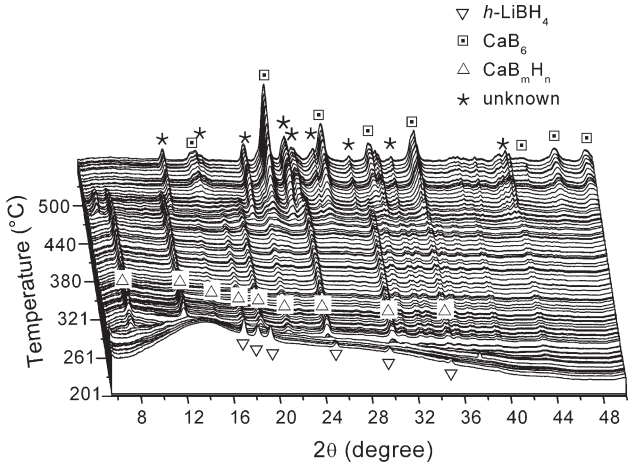

Figure 7. In situ SR-PXD patterns of $0.8LiBH_4 + 0.2Ca(BH_4)_2$ up to 550 °C. CaB_mH_n appears at ca. 235 °C and persists as high as 495 °C. CaB_6 starts to be seen at ca. 440 °C and rapidly grows. Several unknown peaks are found in the final decomposed state.

For both composites, a new set of diffraction peaks appear around 230 °C growing from the melt or from remaining δ-$Ca(BH_4)_2$. TGA and MS data in Figure 9 show that mass decrease and hydrogen release is associated with the formation of this phase. The same set of peaks are seen in $Ca(BH_4)_2 + 0.02NbF_5$ system (not presented here). Therefore the new phase is assumed to be partially dissociated $Ca(BH_4)_2$. We tentatively

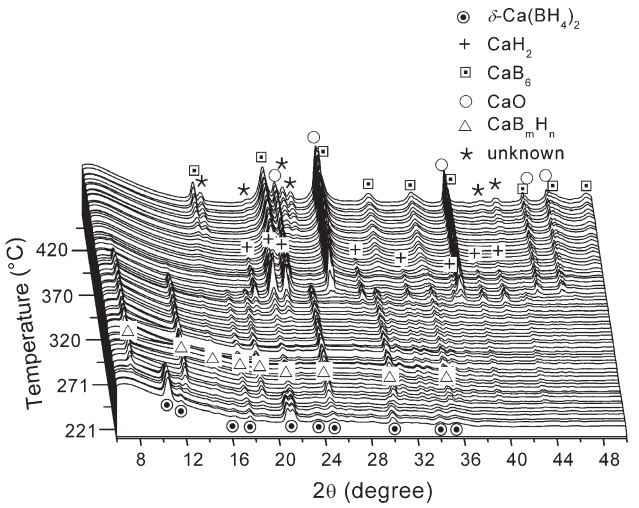

Figure 8. In situ SR-PXD patterns of $0.6LiBH_4 + 0.4Ca(BH_4)_2$ up to 460 °C. A similar set of Bragg peaks as shown in Figure 7 appears at ca. 225 °C. δ-$Ca(BH_4)_2$ coexists with CaB_mH_n, but soon disappears at ca. 245 °C. Bragg peaks from CaB_mH_n disappear at lower temperature (~385 °C) as compared to the composite $0.8LiBH_4 + 0.2Ca(BH_4)_2$. CaB_6 appears at ca. 370 °C and grows while consuming CaH_2. Majority of CaH_2 disappears at ca. 400 °C, but a small trace remains up to ca. 450 °C. The final product from the decomposition is CaB_6 and unknown phases.

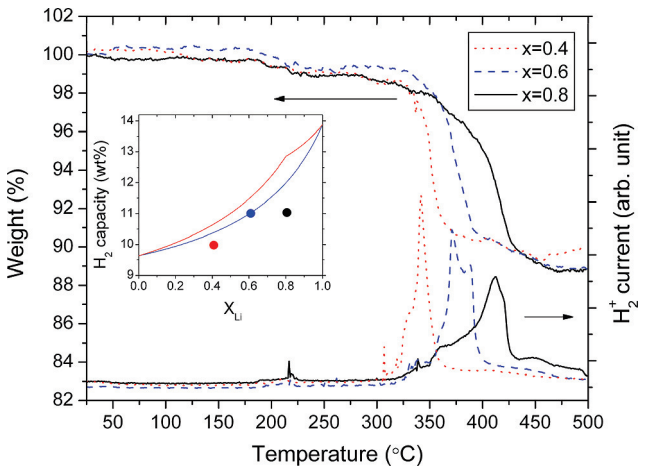

Figure 9. TGA-MS data of $xLiBH_4 + (1 - x)Ca(BH_4)_2$ samples for $x = 0.4$, 0.6, and 0.8. A small amount of hydrogen is released right after the melting, which seems to correspond to the formation of CaB_mH_n. The temperature of the major dissociation reaction becomes higher as x increases. The measured (dots) and the theoretical hydrogen capacities (solid lines) are compared in the inset.

call it as "CaB_mH_n." It is worth noting that CaH_2 is not formed simultaneously with CaB_mH_n, suggesting that this is different from dodecaborohydride ($CaB_{12}H_{12}$) previously described as an intermediate state of dehydrogenated tetraborohydride.[17,39,40] A recent structure analysis of an unknown intermediate phase identified another partially decomposed phase as CaB_2H_2,[38] which is consistent with our observation that the formation of CaB_mH_n is not accompanied by CaH_2. However, the ex situ XRD pattern of the partially decomposed $Ca(BH_4)_2$[33,34,38] is different from that of CaB_mH_n observed by in situ SR-PXD in this study. Nevertheless the recent identification of CaB_2H_2[38] together with our result leads us to the conclusion that partially decomposed $Ca(BH_4)_2$ may have stoichiometry different from $CaB_{12}H_{12}$.

Compared to previous investigations of pure $Ca(BH_4)_2$, a temperature at which CaB_mH_n starts to appear is lower by ~100 °C. In a wide temperature range, this phase is the only crystalline

phase detected by XRD since $LiBH_4$ and $Ca(BH_4)_2$ exist in a melt. The new phase CaB_mH_n forms at ca. 230 °C and the intensity of the Bragg reflections appear to remain constant upon further heating. TGA and MS data (Figure 9) show a similar trend; there is no gradual weight loss or hydrogen release upon further heating of the sample. In a thermodynamic point of view, increasing temperatures should favor the formation of CaB_mH_n and $Ca(BH_4)_2$ and CaB_mH_n should not coexist. One may argue that $Ca(BH_4)_2$ could have transformed completely to CaB_mH_n and only $LiBH_4$ would remain in the melt. However, XRD data in Figure 8 show that the intensity of the CaB_mH_n peaks remain almost constant when the intensity of the CaH_2 peaks increase abruptly. This suggest that CaH_2 is mainly formed from a decomposition of $Ca(BH_4)_2$ remaining as a melt as shown in reaction scheme 3. Therefore, apparently $Ca(BH_4)_2$ only partially transforms to CaB_mH_n, which tends to suggest that the free energy change involved in the formation of CaB_mH_n might be almost zero and the activation barrier might be high, so that the experimental conditions are different from the thermodynamic equilibrium condition. Structural disorder introduced by the melting process may provide a decomposition pathway with a lower activation energy, thereby assisting the formation of CaB_mH_n at around the melting point.

For $x = 0.6$ (Figure 8), CaH_2 peaks appear around 320 °C but shrink rapidly upon the formation of CaB_6. It is natural to think that the reaction 2 immediately follows the reaction 3, that is, $Ca(BH_4)_2$ dissociates first and the product CaH_2 reacts with $LiBH_4$ forming LiH and CaB_6. LiH though is not observed in SR-PXD patterns, possibly due to its weak scattering efficiency. The composite system at $x = 0.8$ (Figure 7) behaves slightly different, that is, no clear signature of CaH_2 is observed. It could be that the lower activity of $Ca(BH_4)_2$ at $x = 0.8$ raises the temperature of the reaction 3, resulting in reaction 2 and 3 or in reaction 4 occurring almost at the same time. It is difficult to know whether the overall dissociation proceeded in two steps or in a single step.

In both cases, there are some unidentified diffraction peaks in the final product, which indicate the presence of more than one unidentified phase since these sets of peaks are different for $x = 0.8$ and $x = 0.6$. Second, compounds like $LiB_{12}H_{12}$ and other unidentified phases that are not easily detected by XRD may form.[17,41] The formation of unidentified phases and CaB_mH_n results in a decomposition route different from the ideal reaction scheme 4. Since CaB_mH_n appear to have higher thermal stability than $Ca(BH_4)_2$, the amount of CaH_2 presumably would not be sufficient to react completely with $LiBH_4$ when $x = 0.8$. Even at $x = 0.6$, CaH_2 appears to be completely consumed by $LiBH_4$, which means that an even larger amount of $Ca(BH_4)_2$ would be required for complete dissociation of $LiBH_4$ through the reaction 2. Lastly, we would like to note that our system has never reached a thermodynamic equilibrium, which is always the case when an experiment is done under continuous heating condition. Since each reaction scheme has different activation barrier, one may find a different reaction sequence when slower or faster heating rate is applied.

3.4. Hydrogen Storage Capacity. The theoretical limit for the hydrogen capacity can be calculated by the combination of two reactions when intermediate compounds are excluded. The lower boundary is set by a linear combination of the reactions 1 and 3; the upper boundary is set by a linear combination of reactions 2 and 3. In the inset of Figure 9, the calculated hydrogen capacity for each limit is drawn in red and blue line for the upper and the lower bound, respectively. This can be taken as a rough estimate, since we in this work show that the decomposition of the composite system is more complex. But, in fact the measured hydrogen storage capacities (TGA, see Figure 9) compare well with the theoretical limits and about 10 wt % of hydrogen are released below 400 °C for $x = 0.4$ and 0.6. This places the composite $x LiBH_4+(1-x)Ca(BH_4)_2$ among the materials with the highest hydrogen storage capacities.

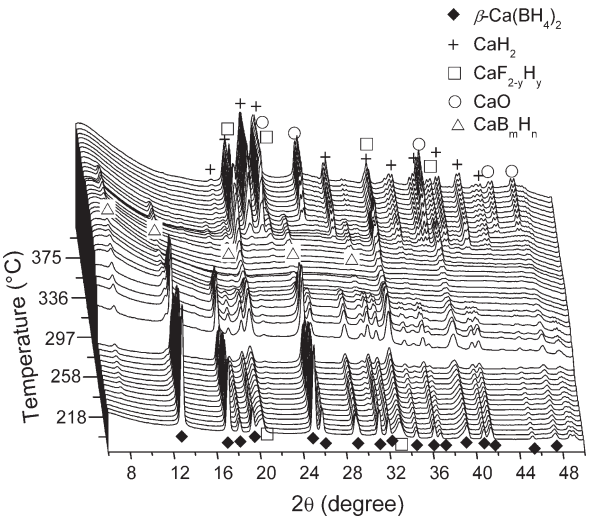

Figure 10. In situ SR-PXD patterns of $0.4LiBH_4 + 0.6Ca(BH_4)_2 + 0.02NbF_5$ up to 400 °C. CaH_2 appears at ca. 340 °C and remains as a main decomposition product. CaB_mH_n appears at ca. 210 °C and disappears at ca. 370 °C. Diffraction from β-$Ca(BH_4)_2$ decrease rapidly accompanied by growth of neither CaB_mH_n nor CaH_2, indicating that β-$Ca(BH_4)_2$ melts rather than decomposes. CaB_6 is not clearly visible. No unknown phases are seen after dissociation. At this composition, dissociation completes at relatively lower temperature as predicted by DSC in Figure 2.

3.5. Reversibility. We have tested reversibility for the composite $0.4LiBH_4 + 0.6Ca(BH_4)_2$, which decomposes at relatively low temperature compared to other compositions. It has been found previously that the reactions 2 and 3 are difficult to reverse without the presence of a catalyst.[9,18,42,43] Therefore, the catalytic additive NbF_5 was added in order to promote the kinetics of release and uptake of hydrogen. Initially, the sample $0.4LiBH_4 + 0.6Ca(BH_4)_2 + 0.02NbF_5$ was heated to 400 °C (heating rate 5 °C/min) and kept at 400 °C for two hours at $p(H_2) = 1$ bar in order to complete the dehydrogenation. In situ SR-PXD patterns were collected and are shown in Figure 10. In this case, no unknown phases were observed after decomposition in contrast to the two other compositions $x = 0.8$ and 0.6. The temperature was still kept constant at 400 °C but the hydrogen pressure was raised to 120 bar in order to study the rehydrogenation in situ as shown in Figure 11. In the beginning, the major phases are CaH_2, $CaF_{2-y}H_y$,[44] and CaO. Gradually, the intensity of the CaH_2 peaks decreases due to hydrogen uptake, but neither $LiBH_4$ nor $Ca(BH_4)_2$ appears since they form a melt. The rehydrogenation at prolonged time also induces particle growth, that is, the broad peaks of CaB_6[28] become visible after a few hours. A TGA-MS experiment was also performed under similar conditions as used above for in situ SR-PXD (see Figure 12). The regenerated *o*-$LiBH_4$ and α-$Ca(BH_4)_2$ prove that this composite system is partially reversible. To our knowledge, this is the first case of reversible mixed cation borohydride system at moderate conditions, 400 °C and $p(H_2) = 90$ bar. TGA data in the inset in Figure 12 shows that about 40% of the hydrogen content is reversibly absorbed after one cycling. The mixing ratio, catalyst, and de/rehydrogentaion condition need to be further optimized in order to achieve better performance.

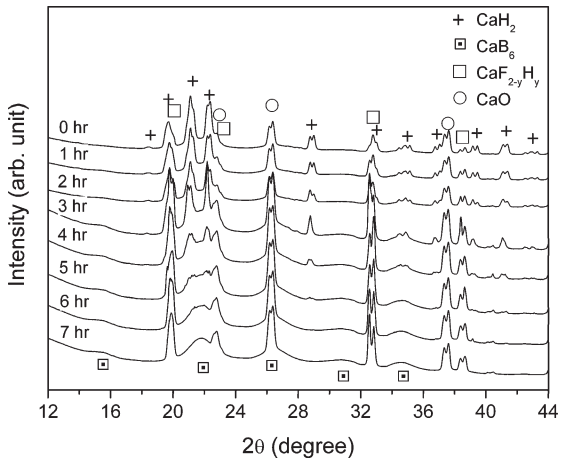

Figure 11. In situ SR-PXD patterns of $0.4LiBH_4 + 0.6Ca(BH_4)_2 + 0.02NbF_5$ at 400 °C, $p(H_2) = 120$ bar. Diffraction from CaH_2 shrinks during the process, but no new peaks appear, suggesting that $LiBH_4$ and $Ca(BH_4)_2$ directly form in the melt. CaB_6 becomes more visible after few hours.

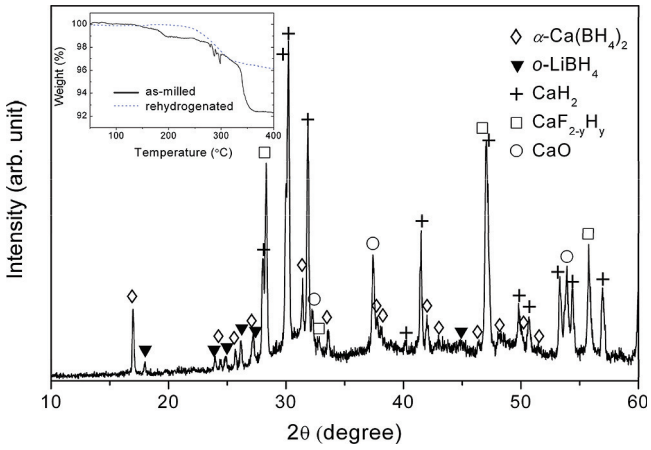

Figure 12. XRD pattern of a sample of $0.4LiBH_4 + 0.6Ca(BH_4)_2 + 0.02NbF_5$, which was dehydrogenated at 400 °C for 2 h under static vacuum and then rehydrogenated at 400 °C, $p(H_2) = 90$ bar for 20 h. The rehydrogenation was not complete, but the formation of *o*-$LiBH_4$ and α-$Ca(BH_4)_2$ clearly proves that this composite system is thermodynamically reversible. TGA data of the as-milled and the rehydrogenated samples are shown in the inset.

4. Conclusions

A systematic study has been carried out on a mixed cation borohydride system, $xLiBH_4 + (1 - x)Ca(BH_4)_2$. The two borohydrides do not react when mixed by a ball-milling but exist as a physical mixture. This mixture exhibits eutectic melting as similar to other pseudobinary systems which have limited mutual solubility in solid state. The eutectic composition lies between $x = 0.6$ and 0.8. The decomposition proceeds in multiple steps and the major reactions are identified by in situ SR-PXD. Right above the eutectic melting point, $Ca(BH_4)_2$ decomposes partially to an unidentified new material CaB_mH_n. At higher temperatures the remaining $Ca(BH_4)_2$ dissociates forming CaH_2, which reacts with molten $LiBH_4$. Hence, hydrogen release does not occur in a single step through a direct reaction between $LiBH_4$ and $Ca(BH_4)_2$ as originally envisioned, but at a certain composition ($x \approx 0.4$) the mixture releases hydrogen at lower temperatures as compared to the individual borohydrides, highlighting the needs for further in-depth investigation of this interesting system. Partial reversibility of the composite is confirmed, which is the first case of mixed cation borohydride systems. In addition, phase transition sequence between the four different $Ca(BH_4)_2$ polymorphs, $\alpha \rightarrow \gamma \rightarrow \beta \rightarrow \delta$, is clearly observed in this in situ SR-PXD study.

Acknowledgment. The authors at KIST acknowledge financial support from the Hydrogen Energy R&D Center, one of the 21st Century Frontier R&D Programs funded by the Ministry of Education, Science, and Technology of Korea. D.R. and T.J. thank the Danish Natural Science Research Council under the program DanScatt and the Carlsberg Foundation for financial support.

References and Notes

(1) Orimo, S.; Nakamori, Y.; Eliseo, J. R.; Züttel, A.; Jensen, C. M. *Chem. Rev.* **2007**, *107*, 4111.
(2) Hauback, B. C. *Z. Kristallogr.* **2008**, *223*, 636.
(3) Mauron, P.; Buchter, F.; Friedrichs, O.; Remhof, A.; Bielmann, M.; Zwicky, C. N.; Züttel, A. *J. Phys. Chem. B* **2008**, *112*, 906.
(4) Au, M.; Jurgensen, A. *J. Phys. Chem. B* **2006**, *110*, 7062.
(5) Mosegaard, L.; Møller, B.; Jørgensen, J.-E.; Filinchuk, Y.; Cerenius, Y.; Hanson, J. C.; Dimasi, E.; Besenbacher, F.; Jensen, T. R. *J. Phys. Chem. C* **2008**, *112*, 1299.
(6) Fang, Z. Z.; Wang, P.; Rufford, T. E.; Kang, X. D.; Lu, G. Q.; Cheng, H. M. *Acta Mater.* **2008**, *56*, 6257.
(7) Gross, A. F.; Vajo, J. J.; Van Atta, S. L.; Olson, G. L. *J. Phys. Chem. C* **2008**, *112*, 5651.
(8) Vajo, J. J.; Skeith, S. L.; Mertens, F. *J. Phys. Chem. B* **2005**, *109*, 3719.
(9) Yang, J.; Sudik, A.; Wolverton, C. *J. Phys. Chem. C* **2007**, *111*, 19134.
(10) Bösenberg, U.; Doppiu, S.; Mosegaard, L.; Barkhordarian, G.; Eigen, N.; Borgschulte, A.; Jensen, T. R.; Cerenius, Y.; Gutfleisch, O.; Klassen, T.; Dornheim, M.; Bormann, R. *Acta Mater.* **2007**, *55*, 3951.
(11) Nakamori, Y.; Miwa, K.; Ninomiya, A.; Li, H.-W.; Ohba, N.; Towata, S.; Züttel, A.; Orimo, S. *Phys. Rev. B* **2006**, *74*, 045126.
(12) Ravnsbæk, D.; Filinchuk, Y.; Cerenius, Y.; Jakobsen, H. J.; Besenbacher, F.; Skibsted, J.; Jensen, T. R. *Angew. Chem. Int. Ed.* **2009**, accepted.
(13) Li, H.-W.; Orimo, S.; Nakamori, Y.; Miwa, K.; Ohba, N.; Towata, S.; Züttel, A. *J. Alloys Compd.* **2007**, *446*, 315.
(14) Nickels, E. A.; Jones, M. O.; David, W. I. F.; Johnson, S. R.; Lowton, R. L.; Sommariva, M.; Edwards, P. P. *Angew. Chem., Int. Ed.* **2008**, *47*, 2817.
(15) Xiao, X.-B.; Yu, W.-Y.; Tang, B.-Y. *J. Phys.: Condens. Matter* **2008**, *20*, 6.
(16) Hagemann, H.; Longhini, M.; Kaminski, J. W.; Wesolowski, T. A.; Černý, R.; Penin, N.; Sørby, M. H.; Hauback, B. C.; Severa, G.; Jensen, C. M. *J. Phys. Chem. A* **2008**, *112*, 7551.
(17) Hwang, S. J.; Bowman, R. C.; Reiter, J. W.; Rijssenbeek, J.; Soloveichik, G. L.; Zhao, J. C.; Kabbour, H.; Ahn, C. C. *J. Phys. Chem. C* **2008**, *112*, 3164.
(18) Pinkerton, F. E.; Meyer, M. S. *J. Alloys Compd.* **2008**, *464*, L1.
(19) Jin, S.-A.; Lee, Y.-S.; Shim, J.-H.; Cho, Y. W. *J. Phys. Chem. C* **2008**, *112*, 9520.
(20) Kim, J.-H.; Jin, S.-A.; Shim, J.-H.; Cho, Y. W. *Scr. Mater.* **2008**, *58*, 481.
(21) Rönnebro, E.; Majzoub, E. H. *J. Phys. Chem. B* **2007**, *111*, 12045.
(22) Cerenius, Y.; Ståhl, K.; Svensson, L. A.; Ursby, T.; Oskarsson, Å.; Albertsson, J.; Liljas, A. *J. Synchrotron Rad.* **2000**, *7*, 203.
(23) Ravnsbæk, D.; Mosegaard, L.; Jørgensen, J.-E.; Jensen, T. R. Proceedings of the 29th Risø International Symposium on Materials Science: Energy Materials - Advances in Characterization, Modelling and Application, 2008.
(24) Hammersley, A. P.; Svensson, S. O.; Hanfland, M.; Fitch, A. N.; Häusermann, D. *High Pressure Res.* **1996**, *14*, 235.
(25) Miwa, K.; Aoki, M.; Noritake, T.; Ohba, N.; Nakamori, Y.; Towata, S.; Züttel, A.; Orimo, S. *Phys. Rev. B* **2006**, *74*, 155122.
(26) Buchter, F.; Łodziana, Z.; Remhof, A.; Friedrichs, O.; Borgschulte, A.; Mauron, P.; Züttel, A.; Sheptyakov, D.; Barkhordarian, G.; Bormann, R.; Chłopek, K.; Fichtner, M.; Sørby, M.; Riktor, M.; Hauback, B.; Orimo, S. *J. Phys. Chem. B* **2008**, *112*, 8042.
(27) Majzoub, E. H.; Rönnebro, E. *J. Phys. Chem. C* **2009**, *113*, 3352.
(28) Kim, Y.; Reed, D.; Lee, Y.-S.; Lee, J. Y.; Shim, J.-H.; Book, D.; Cho, Y. W. *J. Phys. Chem. C* **2009**, *113*, 5865.
(29) Züttel, A.; Wenger, P.; Rentsch, S.; Sudan, P.; Mauron, P.; Emmenegger, C. *J. Power Sources* **2003**, *118*, 1.
(30) Filinchuk, Y.; Chernyshov, D.; Dmitriev, V. *Z. Kristallogr.* **2008**, *223*, 649.

(31) Filinchuk, Y.; Chernyshov, D.; Cerny, R. *J. Phys. Chem. C* **2008**, *112*, 10579.

(32) Riktor, M. D.; Sørby, M. H.; Chłopek, K.; Fichtner, M.; Buchter, F.; Züttel, A.; Hauback, B. C. *J. Mater. Chem.* **2007**, *17*, 4939.

(33) Kim, J.-H.; Jin, S.-A.; Shim, J.-H.; Cho, Y. W. *J. Alloys Compd.* **2008**, *461*, L20.

(34) Aoki, M.; Miwa, K.; Noritake, T.; Ohba, N.; Matsumoto, M.; Li, H.-W.; Nakamori, Y.; Towata, S.; Orimo, S. *Appl. Phys. A* **2008**, *92*, 601.

(35) Fichtner, M.; Chłopek, K.; Longhini, M.; Hagemann, H. *J. Phys. Chem. C* **2008**, *112*, 11575.

(36) Filinchuk, Y.; Rönnebro, E.; Chandra, D. *Acta Mater.* **2009**, *57*, 732.

(37) Lee, Y.-S.; Kim, Y.; Cho, Y. W.; Shapiro, D.; Wolverton, C.; Ozolins, V. *Phys. Rev. B* **2009**, *79*, 104107.

(38) Riktor, M. D.; Sørby, M. H.; Chłopek, K.; Fichtner, M.; Hauback, B. C. *J. Mater. Chem.* [Online early access]. DOI: 10.1039/b818127f.

(39) Matsunaga, T.; Buchter, F.; Mauron, P.; Bielman, A.; Nakamori, Y.; Orimo, S.; Ohba, N.; Miwa, K.; Towata, S.; Züttel, A. *J. Alloys Compd.* **2008**, *459*, 583.

(40) Ozolins, V.; Majzoub, E. H.; Wolverton, C. *J. Am. Chem. Soc.* **2009**, *131*, 230.

(41) Mosegaard, L.; Møller, B.; Jørgensen, J.-E.; Bösenberg, U.; Dornheim, M.; Hanson, J. C.; Cerenius, Y.; Walker, G.; Jakobsen, H. J.; Besenbacher, F.; Jensen, T. R. *J. Alloys Compd.* **2007**, *446*−*447*, 301.

(42) Barkhordarian, G.; Klassen, T.; Dornheim, M.; Bormann, R. *J. Alloys Compd.* **2007**, *440*, L18.

(43) Lim, J.-H.; Shim, J.-H.; Lee, Y.-S.; Cho, Y. W.; Lee, J. *Scr. Mater.* **2008**, *59*, 1251.

(44) Kim, J.-H.; Shim, J.-H.; Cho, Y. W. *J. Power Sources* **2008**, *181*, 140.

JP904400B